COBEM 2023 27TH INTERNATIONAL CONGRESS OF MECHANICAL ENGENEERING

ABCM Brazilian Society of Mechanical Sciences and Engineering
27th ABCM International Congress of Mechanical Engineering
December 04-08, 2023, Florianópolis-SC, Brazil

COB-2023-1151
0D/1D ANALYSIS OF THE PERFORMANCE AND EMISSIONS OF A NATURAL GAS ENGINE OPERATING ON ETHANOL

Miguel Humberto Barrientos Sandoval
miguel.sandoval@labmci.ufsc.br
Gabriel de Andrade Janene Gonini
gabriel.gonini@labmci.ufsc.br
Javier Antonio Mendoza Corredor
javier.mendoza@labmci.ufsc.br
Milton Keisy Kouketsu
milton.kouketsu@labmci.ufsc.br
Leonel R. Cancino
leonel.cancino@labmci.ufsc.br
Internal Combustion Engines Laboratory - Joinville Technological Center - Federal University of Santa Catarina - LABMCI/CTJ/UFSC.
Rua Dona Francisca 8300, Joinville, SC, CEP 89219-600, Brazil.

Amir Antonio Martins Oliveira Jr.
amir.oliveira@ufsc.br
Combustion and Thermal Systems Engineering Laboratory - Technological Center - Federal University of Santa Catarina - LABCET/EMC/CTC/UFSC,.
Trindade, Florianópolis, SC, CEP 88040-900, Brazil.

Abstract. *This work presents a comprehensive numerical analysis of an internal combustion engine (ICE) using a 0D/1D simulation approach. The analysis focuses on simulating a natural gas-fueled stationary engine for electricity generation (Vortec 3.0 - LW6) operating with ethanol. The study includes an in-depth investigation of engine performance parameters such as power, torque, and brake-specific fuel consumption (BSFC), as well as engine emissions including nitrogen oxides (NO_X), hydrocarbons (HC), and carbon monoxide (CO). Furthermore, the procedure used to characterize the engine's geometric parameters, dimensions, valve lift curves, and other necessary details for the 0D/1D simulations is described. For the combustion process, the Vibe 2-Zone combustion model is used together with literature data to define the function parameters for the analyzed fuels. In addition, models provided by AVL-BOOST™are used to describe the formation of the combustion product emissions of natural gas and ethanol, respectively. The obtained results show a clear difference in engine performance based on the type of fuel. Specifically, in the case of the engine operating with ethanol, a significant increase in output power is observed compared to the engine running on natural gas. However, the use of ethanol results in a significant increase in specific fuel consumption due to its lower heating value and lower air/fuel ratio. Furthermore, the analysis demonstrates that the use of ethanol allows for a reduction in NO_X emissions across the entire analyzed rotational range due to lower combustion temperatures. However, higher HC and CO emissions are observed. Overall, the study provides valuable insights into the performance and emissions of the engine when operating with natural gas and ethanol. The results can be used to optimize the design and operation of the engine to achieve the desired balance between efficiency and emissions in various applications.*

Keywords: *Internal combustion engines, 0D/1D simulation, Combustion, AVL BOOST™*

1. INTRODUCTION

The increase in greenhouse gas emissions has become one of the main global concerns due to its social and environmental impact. In an attempt to address this problem, various governmental entities have implemented environmental policies to regulate and ensure the reduction of pollutant gases. However, efforts to meet environmental requirements have been insufficient, resulting in increasingly high levels of greenhouse gas emissions (STATISTA, 2023).

With the aim of reducing and mitigating these impacts, the automotive industry has been developing different strategies and technologies in internal combustion engines, seeking to produce mechanical power in a cleaner and more sustainable manner. Among the developed strategies, the use of lean mixtures, downsizing, turbocharging, increased compression ratio, and the use of alternative fuels stand out, among others (Amaral *et al.*, 2021). Among these strategies, the use of alternative fuels has gained significant acceptance since, in addition to reducing pollutant emissions, they allow for power generation with combustion characteristics similar to gasoline engines (Semin, 2008), (Poudel and Deb, 2017).

One of the most commonly used alternative fuels is ethanol, which is produced and commercially available on a large scale in different countries. Compared to gasoline, the combustion of ethanol in internal combustion engines presents advantages both in economic terms and in terms of pollutant emissions (Iliev, 2015). According to the literature, the use of ethanol results in cleaner combustion with reduced CO and NO_X emissions, although it leads to increased HC emissions due to lower flame temperatures (Masum *et al.*, 2013). However, due to its lower calorific value, ethanol results in lower power output. Direct comparisons of natural gas combustion in internal combustion engines with ethanol combustion are not widely found in the literature, making the direct analysis of these fuels challenging.

Given this scenario, this study aims to evaluate the combustion characteristics and emissions of natural gas engines converted to run on ethanol through 0D/1D simulations. For this purpose, experimental data from a Vortec 3.0 (LW6) engine provided by the manufacturer are used, as well as geometric parameters collected directly from the engine. The simulations are performed using the Vibe 2-Zone combustion model, along with the San Diego UCSD (2016) and Marinov Marinov (1999) thermodynamic database to describe the combustion process of natural gas and ethanol, respectively. It is important to note that the simulations are performed at chemical equilibrium and no reaction rates or kinetic effects over time are considered. However, the San Diego and Marinov thermodynamic databases are used to specify the chemical species present in the fuel. Additionally, models provided by AVL-BOOST™ are used to characterize HC, CO, and NO_X emissions.

2. THEORETICAL BACKGROUND

In this section, the literature works and numerical models that contribute to the development of the research are presented. The bibliography is summarized in Table 1.

2.1 Review of the Literature.

The performance and emissions of internal combustion engines operating with ethanol and natural gas have been extensively analyzed in several numerical and experimental studies. However, comparison of natural gas combustion with ethanol combustion is not widely found in the literature, which makes direct analysis of these fuels difficult. Table 1 presents studies evaluating brake power, BSFC and emissions from engines operating on natural gas and ethanol at different operating conditions. In addition, studies evaluating these same parameters in relation to the gasoline engine are also presented. In the table, the arrows indicate the variation of the first fuel in relation to the second. For example, in the first row, the downward arrow (↓) indicates that the power, BSFC and HC, CO, CO_2 and NO_X emissions of the natural gas engine decreased compared to the gasoline engine.

Table 1. Previous research on the effects of ethanol and natural gas on combustion parameters and emissions.

Type of engine, reference	CR	Engine speed (rpm)	Fuel	Brake power	BSFC	HC	CO	CO_2	NOx
Four-cylinder SI engine, four stroke (1.5 L), (Geok *et al.*, 2009)	9.2:1	1500 to 5000	CGN, Gasoline	↓	↓	↓	↓	↓	-
Four-cylinder SI engine, four Stroke at Full load (1.5 L), (Aslam *et al.*, 2006)	9.2:1	1500 to 5500	CGN, Gasoline	↓	↓	↓	↓	↓	↑
Four-cylinder SI engine, four Stroke (2.0 L), (Aldhaidhawi *et al.*, 2020)	8.5:1 to 16.5:1	2500	Ethanol, Gasoline	↓	↑	↓	↓	-	↓
Single-cylinder SI engine, four-stroke (Full throttle), (Balki *et al.*, 2014)	8.5:1	1600 to 3600	Ethanol, Gasoline	-	↑	↓	↓	↑	↓
single-cylinder, four-stroke, spark ignited Cooperative Fuel Research (CFR) engine at different fuel-air equivalence (Ran *et al.*, 2019)	8:1	1200	Ethanol, Natural gas	-	-	↓	↓	-	↓
single-cylinder, four-stroke, spark ignited Cooperative Fuel Research (CFR) engine at different fuel-air equivalence (Ran *et al.*, 2020)	9:1 to 11:1	1200	Ethanol, Natural gas	-	-	↑	↑	-	↓

As observed, the use of ethanol tends to reduce HC, CO and NO_X emissions compared to the gasoline engine. However, it presents a reduction in power output and an increase in BSFC. Similarly, it can be observed that natural gas tends to reduce brake power, BSFC and HC and CO emissions. However, it shows an increase in NO_X emissions. Specifically,

when comparing ethanol with natural gas, differences in HC and CO emissions were found in the papers presented. However, it should be noted that the results presented were dependent on the compression ratios and the range of air/fuel ratio analyzed.

3. METHODOLOGY

In this section, we present the methodology implemented for extracting the geometric data of the engine, as well as the setup conducted for the development of this work. Additionally, the combustion and emission models used in the simulations are described.

To obtain the geometric data of the engine, a meticulous extraction of information was carried out, including dimensions and valve lift curves. As for the work setup, a set of initial and boundary conditions reflecting the engine's operating environment was established. These conditions include ambient temperature, atmospheric pressure, compression ratio, and other relevant parameters. Finally, the Vibe 2-Zone combustion model is described, which allows the representation of the combustion process in the engine cylinders.

3.1 Engine specifications and geometrical characteristics

As mentioned, the simulations of the engine operating with natural gas and ethanol will be performed on a Vortec 3.0 (LW6) engine. The main characteristics of the engine are presented in Table 2.

Table 2. Engine technical specifications.

Engine parameters	Description	Engine parameters	Description
Total displacement volume	2966.59 cm^3	Compression ratio	10.5;1
Bore x Stroke	(101.60 x 91.44) mm	Maximum power	54 kW (73 hp) a 2200 rpm
Number of cylinders	4	Maximum torque	241 N.m (178 lb-ft) a 1600 rpm
Valves per cylinder	2	Maximum engine speed	2200 rpm

In the development of the 0D/1D simulations, it was necessary to obtain and characterize the geometric information of the engine, which was not found in the manufacturer's catalog. Specifically, the volume of the intake and exhaust manifolds, as well as the dimensions and lift profile of the intake and exhaust valves, were determined through direct measurements.

To determine the volume of the manifolds, two approaches were used. Initially, the volume was measured by introducing a liquid into the intake and exhaust manifolds. These measurements were performed with a series of repetitions and later compared to the data obtained from 3D scanning of the parts. It is worth noting that the scanning was carried out after the pre-preparation of the cylinder head, which involved the disassembly of the intake and exhaust valves, as well as cleaning of the part. The same methodology was applied to characterize part of the volume of the manifolds present in the engine's cylinder head. Next, the dimensions of the rocker arm and the intake and exhaust valves were determined. For this purpose, a Mitutoyo coordinate measuring machine was used, which determined the profile and dimensions of these components with high precision. The dimensions of the rocker arm were used to calculate the maximum lift of the valves, while the valve profiles were used to dimension these components using SOLIDWORKS software. Figure 1 shows the measurement procedures mentioned above.

Finally, the intake and exhaust camshafts were characterized and dimensioned to determine the lift profile of the valves. Two measurement techniques were used for this purpose. In the first technique, the profile of the intake and exhaust camshafts was extracted using the coordinate measuring machine, and subsequently, dimensioned using SOLIDWORKS. In the second technique, the camshaft was taken to a lathe, where measurements were taken degree by degree with the aid of a digital comparator gauge. The measurements were repeated to ensure the accuracy of the results. Subsequently, the two techniques were compared to determine the lift profiles of the valves. Figure 2 illustrates the measurement techniques applied to determine the lift profile of the valves.

3.2 0D/1D simulation setup

Figure 3 presents the zero-dimensional/one-dimensional model of the simulation of the Vortec 3.0 (LW6) engine performed in AVL BOOST™. The developed model features four cylinders (C1 to C4) connected to the intake and exhaust manifolds (PL1 to PL4) and the system boundaries (SB1 and SB2), which define the inlet and outlet conditions of the gases. Additionally, it includes the injector/carburetor (I1), throttle valve (TH1), air filter (CL1), catalytic converter (CAT1), restrictions (R1 to R4), gaskets (J1 to J3), and measurement points (MP1 to MP4). It is important to note that the catalytic converter (CAT1) does not undergo any catalytic process and is only considered for pressure loss in the system.

The simulations were conducted under full-load conditions, maintaining the stoichiometric ratio for each fuel, in a

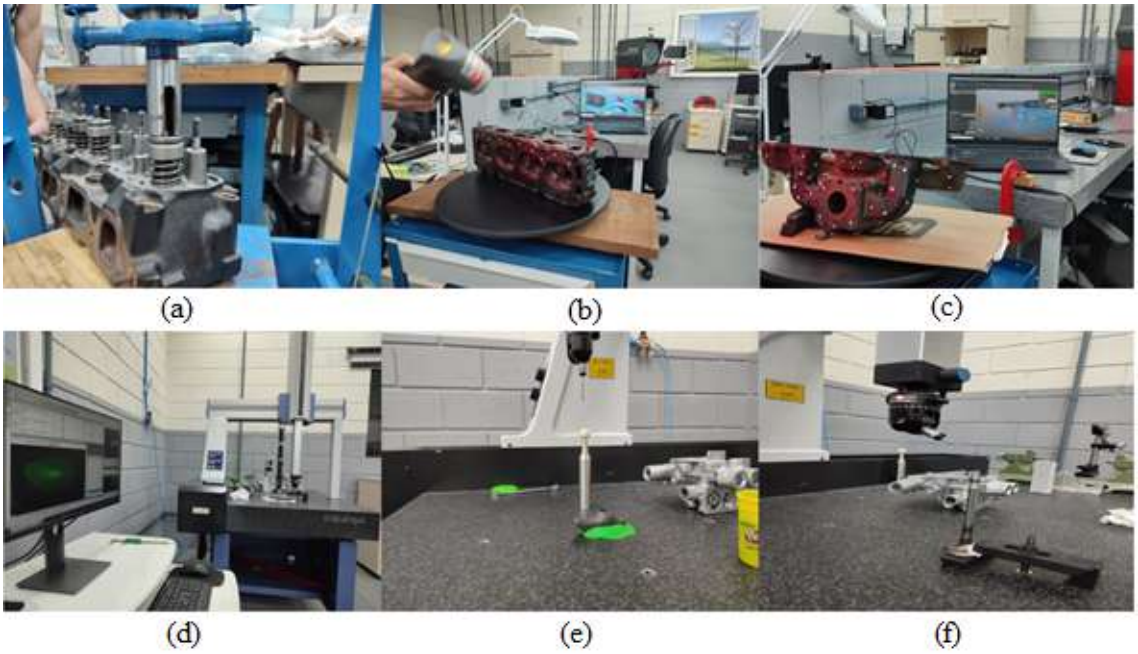

Figure 1. Engine geometry characterization. (a) Disassembly of the intake and exhaust valves, (b,c) 3D scanning of the cylinder head, intake and exhaust manifolds, (d,f,g) characterization of cam, rocker arm, intake and exhaust valve profile using a coordinate measuring machine.

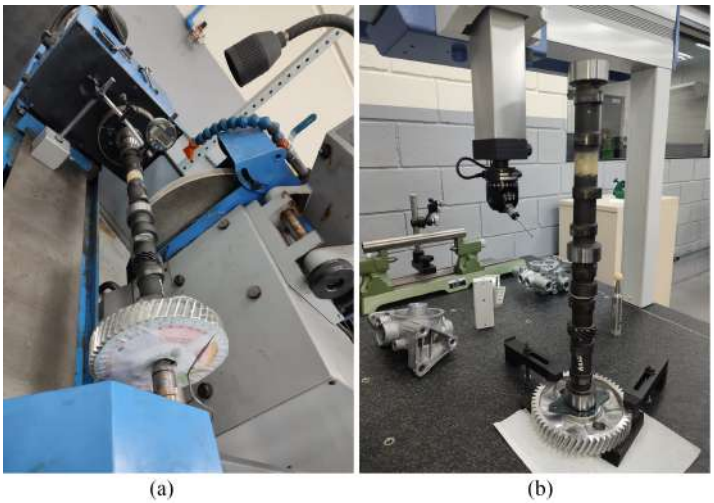

Figure 2. Characterization of the valve lift profile using (a) a digital comparator gauge (b) a coordinate measuring machine.

rotational range of 1300 to 2200 rpm. The Vibe 2-Zone model was used to describe the burned mass fraction, while the heat transfer model was based on the Woschni (1978) model. Furthermore, the Patton *et al.* (1989) model was employed to describe friction losses. In the simulations with ethanol, pure ethanol was considered as fuel. The calorific value of pure ethanol used in these simulations was set at 27733 kJ/kg, according to the thermodynamic data of the database used. On the other hand, in the simulations with natural gas, a specific chemical composition for natural gas was used, which is detailed in the reference work (GASMIG, 2023). For these simulations, the calorific value of natural gas was set at 49402 kJ/kg, following the specifications of this chemical composition and the thermodynamic basis used for natural gas. It is important to note that in AVL BOOST the "control ratio" function was used in the injector element to keep the engine operation at lambda equal to 1 in all operating conditions. Therefore, the fuel mass varied according to the engine rotational speed and the specific conditions of each simulation.

To determine the boundary conditions in the simulations, initial simulations were conducted considering ambient temperature and atmospheric pressure, with variable wall temperature (including piston, cylinder head, cylinder, and exhaust duct walls). From these simulations, temperature data were collected for each component at different rotational points. The obtained average temperatures were subsequently used in the engine simulations under fixed temperature conditions, considering chemical kinetics.

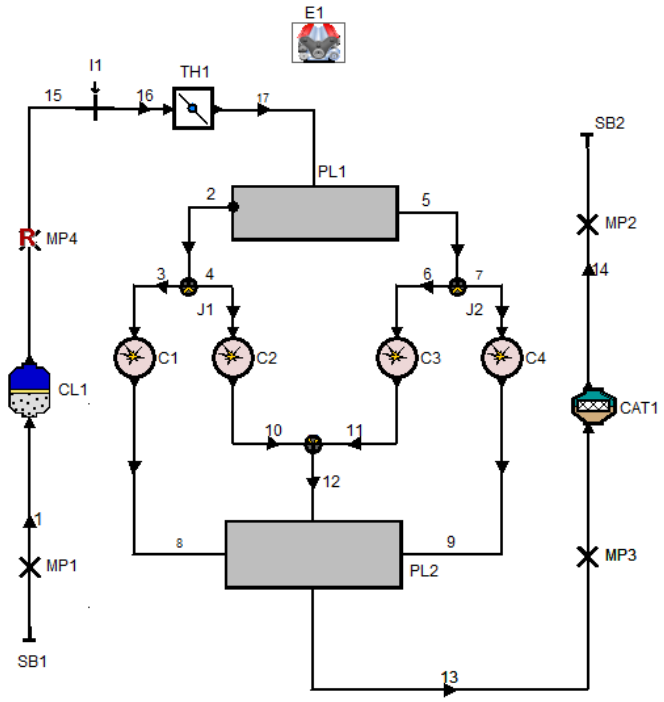

Figure 3. 0D/1D engine model.

3.3 Combustion model

For the combustion characterization, the Vibe 2-Zone model was used. In this model, it is assumed that the combustion chamber is divided into two zones, separating the volume of burned gases from the volume of air/fuel mixture that has not yet ignited (Kesgin, 2004). However, the assumption that the unburned air/fuel mixture and the burned gases have the same temperature is not considered. Instead, the first law of thermodynamics is applied to the burned charge and the unburned charge, respectively (Noske, 1988), (AVL, 2023).

$$\frac{dm_b u_b}{d\alpha} = -P_c \frac{dV_b}{d\alpha} + \frac{dQ_F}{d\alpha} - \sum \frac{dQ_{Wb}}{d\alpha} + h_u \frac{dm_b}{d\alpha} - h_{BB,b} \frac{dm_{BB,b}}{d\alpha} \tag{1}$$

$$\frac{dm_u u_u}{d\alpha} = -P_c \frac{dV_u}{d\alpha} - \sum \frac{dQ_{Wu}}{d\alpha} - h_u \frac{dm_B}{d\alpha} - h_{BB,b} \frac{dm_{BB,b}}{d\alpha} \tag{2}$$

Where dm_u represents the change in internal energy of the cylinder, $P_c \frac{dV}{d\alpha}$ the piston work, $\frac{dQ_f}{d\alpha}$ the heat input from the fuel, $\frac{dQ_W}{d\alpha}$ the heat losses from the walls, $h_u \frac{dm_b}{d\alpha}$ the enthalpy flow from the unburned zone to the burned zone due to the conversion of fresh charge into combustion products, $h_{BB,b} \frac{dm_{BB,b}}{d\alpha}$) the enthalpy due to blow by, and the subscripts "b" and "u" refer to the burned and unburned zones, respectively. It is important to note that the heat flow between the two zones is not considered (AVL, 2023).

3.4 Vibe function estimation

The vibe function is a commonly used expression to represent the burned mass fraction as a function of the crank angle x_b (θ) (Heywood, 2018). The vibe function can be represented as:

$$x_b = 1 - exp[-a(\frac{\theta - \theta_0}{\Delta\theta})^{m+1}] \tag{3}$$

Where, in context, θ_0 represents the start of combustion, $\Delta\theta$ represents the duration of combustion, and the adjustable parameters "a" and "m" commonly referred to as the efficiency parameter and shape factor, respectively, indicate the duration and shape of the combustion curve (Liu and Dumitrescu, 2019). As observed in the equation, the vibe function is highly influenced by the adjustment parameters, as they define the characteristics of the burning rate. For this particular research, the parameters "a" and "m" were obtained from the literature, as reported in (Rufino *et al.*, 2021), (Niculae *et al.*, 2020). Furthermore, it is important to highlight that the ignition timing of the simulations was adjusted to achieve the maximum brake torque, as per (Heywood, 2018).

3.5 Emission model.

For the formation of NO_X, AVL BOOST™ relies on Pattas and Häfner (1973) in conjunction with the well-known Zeldovich mechanism (AVL, 2023). The reactions used in the NO_X formation model are presented in table 3.

Table 3. Rate constants for NO_X formation model.

	Stoichiometry	Rate k_i=$k_{0,i}T^a e^{(\frac{-TA_i}{T})}$	k_0 [cm^3,mol,s]	a[-]	T_A[K]
R1	N_2+*O*=*NO*+*N*	r_1=$k_1 c_{N2} c_O$	4.93*E*13	0.0472	38048.01
R2	O_2+*N*=*NO*+*O*	r_2=$k_2 c_{O2} c_N$	1.48*E*08	1.5	2859.01
R3	*N*+*OH*=*NO*+*H*	r_3=$k_3 c_{OH} c_N$	4.22*E*13	0.0	0.0
R4	N_2O+*O*=*NO*+*NO*	r_4=$k_4 c_{N2O} c_O$	4.58*E*13	0.0	12130.6
R5	O_2+N_2=N_2O+*O*	r_5=$k_5 c_{O2} c_{N2}$	2.25*E*10	0.825	50569.7
R6	*OH*+N_2=N_2O+*H*	r_6=$k_2 c_{OH} c_{N2}$	9.14*E*07	1.148	36190.66

The rate of NO_X production is determined by the aforementioned reactions in conjunction with equations 4, 5, and 6, where the concentration of N_2 O is calculated as (AVL, 2023):

$$c_{N2O} = 1.1802 * 10^{-6} T^{0.6125} e^{(\frac{9471.6}{T})} c_{N2} \sqrt{p_{O2}} \tag{4}$$

And the final *NO* production/destruction rate is calculated as:

$$r_{NO} = C_{PostMult} C_{KinetcMult} 2(1-\alpha^2)(\frac{r_1}{1+\alpha A K_2} + \frac{r_4}{1+AK_4}) \tag{5}$$

With:

$$\alpha = \frac{c_{NO,act}}{c_{NO,equ}} \frac{1}{C_{KineticMult}}; AK_2 = \frac{r_1}{r_2+r_3}; AK_4 = \frac{r_4}{r_5+r_6} \tag{6}$$

Where $C_{PostMult}$ denotes Post-Processing Multiplier, $C_{KineticMult}$ denotes Kinetic Multiplier, C denotes equilibrium molar concentration, and r_i denotes reaction rates of the Zeldovich mechanism. In regard to CO formation, AVL BOOST™ employs a model based on Onorati *et al.* (2001). Table 4 presents the reactions utilized in this model.

Table 4. Reactions for *CO* formation model.

	Stoichiometry	Rate
R1	*CO*+*OH*=CO_2+*H*	r_1=6.76*$10^{10} e^{(T/1102.0)} c_{CO} c_{OH}$
R2	*CO*+O_2=CO_2+*O*	r_2=2.51*$10^{12} e^{(-24055.0)/T)} c_{CO} c_{O2}$

The final CO production/destruction rate is given by:

$$r_{CO} = C_{Const}(r_1 + r_2)(1-\alpha) \tag{7}$$

with

$$\alpha = \frac{c_{(NO,act)}}{c_{(NO,equ)}} \tag{8}$$

For the description of hydrocarbon formation, a model is utilized that takes into account the main sources of formation. The sources of unburned hydrocarbon formation can be observed in detail in Iliev (2015).

4. RESULTS

4.1 Validation of the 0D/1D simulations.

The validation of the zero-unidimensional simulation was performed using the torque and power curves provided by the engine manufacturer at different rotation points. For this, data from the engine natural gas operation literature was used, since the necessary facilities for obtaining data directly from the engine were not available. Figure 4 shows the comparison between the results obtained from the 0D/1D simulation and the experimental data.

In Figure 4 it can be seen that the implemented one-dimensional methodology adequately represents the evolution of the torque and power curve of the motor. The percentage error for both torque and power was less than 1% at the different rotation points analyzed, showing a good correlation between simulations and experimental data.

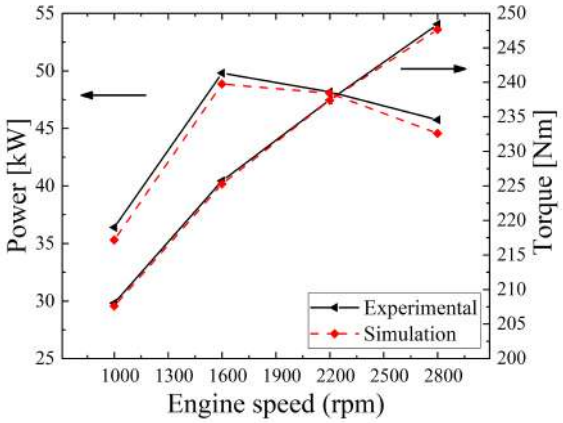

Figure 4. Validation of the 0D/1D engine model operating on natural gas.

4.2 0D/1D analysis of engine performance operating on natural gas and ethanol.

Figure 5 show the power, torque and BSFC of the engine operating with natural gas and ethanol at different rpm points. It should be noted that the compression ratio was kept constant and the temperatures of the piston wall, cylinder head, cylinder, and exhaust duct were determined as described in section 3.2

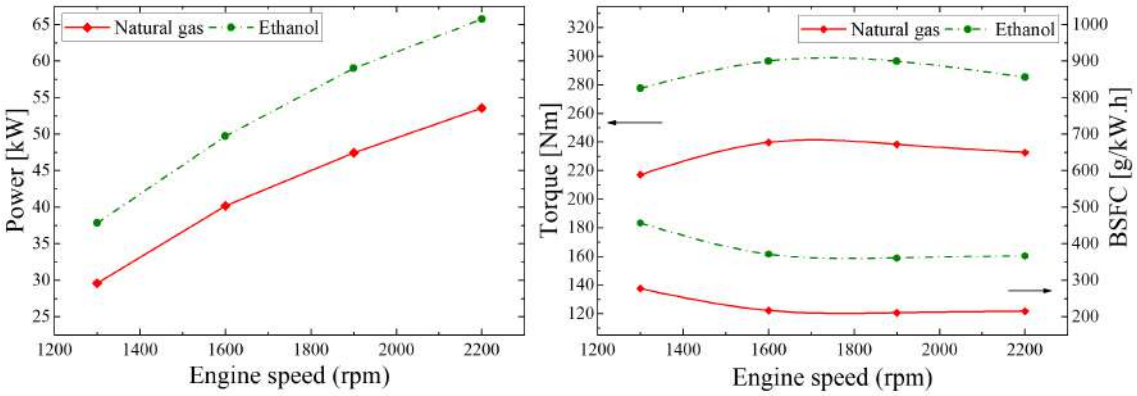

Figure 5. Engine power operating on natural gas and ethanol.

As observed in Figure 5, the use of ethanol results in a significant increase in engine power compared to the original case with natural gas. The increase in power varies from 8.2 kW to 12.1 kW, with the variations being greater at higher rotation speeds. Compared to ethanol, natural gas has a higher calorific value. However, as described by Geok *et al.* (2009), the airflow generated by natural gas in the intake manifold can lead to a decrease in volumetric efficiency and, consequently, a reduction in the power density of the charge injected into the cylinder and the engine power output. Furthermore, Geok *et al.* (2009) and Kustanto *et al.* (2017) state that the increase in power output with increasing rotational speed may be directly related to the slower burning speed of natural gas.

The maximum torque, as presented in Figure 5, was obtained at speeds of 1600 rpm for the different fuels tested, reaching values of 239 N.m for natural gas and 296 N.m for ethanol. The trend shows an increase in torque as the speed increases up to 1600 rpm. From this point on, torque begins to decrease consequently with speed. Similarly, figure 6 shows that the use of ethanol produces a significant increase in BSFC compared to the engine with natural gas. The behavior of ethanol, according to Iliev (2015), is given by its low calorific value and its lower air/fuel ratio, which means that for a specific air/fuel equivalence ratio more fuel (ethanol) is required. The trend shows a decrease in BSFC up to 1600 rpm with slight increases from this point on. At high revs an increase in BSFC can be observed. This increase is mainly characterized, according to Jahirul *et al.* (2010), by the increase in friction power compared to the indicated power.

4.3 Analysis of engine emissions operating with natural gas and ethanol.

Figure 7 displays the NO_X and HC emissions of the engine operating with natural gas and ethanol at different rotational points.

As observed in Figure 7, variations in NO_X emissions between the two fuels were noted at different rotational points. Overall, natural gas demonstrated higher levels of NO_X across all evaluated speed ranges. This behavior can be attributed

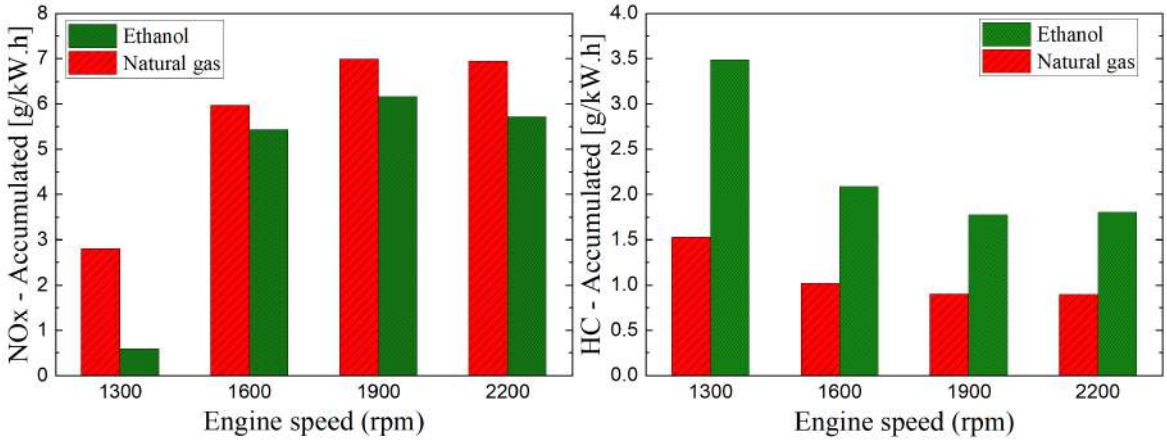

Figure 6. NO_X and HC emissions from the engine operating on natural gas and ethanol.

to the higher heating value of natural gas, resulting in higher combustion temperatures, which favor the formation of NO_X. Similar results have been observed in (Balki *et al.*, 2014), (Aldhaidhawi *et al.*, 2020). Additionally, it was found that NO_X emissions tend to increase for both fuels as engine speed increases. This increase is related to the fact that at higher speeds, the engine reaches higher combustion temperatures, which contribute to the formation of NO_X (Masum *et al.*, 2013).

Regarding HC emissions, ethanol exhibited higher emissions throughout the speed range. This trend is also influenced by the combustion temperature, as demonstrated by Celik (2008). Lower temperatures allow for partial combustion near the combustion chamber walls, resulting in incomplete fuel combustion and an increase in HC emissions. This behavior can be observed under different engine speed conditions, where lower RPM conditions with lower combustion temperatures lead to higher HC emissions. As engine speeds and combustion temperatures increase, HC emissions decrease.

Regarding CO emissions, the simulations conducted showed that the engine operating with ethanol exhibited higher emissions compared to the engine running on natural gas across the entire evaluated speed range. Additionally, it was observed that CO emissions decreased for both fuels as the engine rotational speed increased. The CO emissions obtained for the engine operating with natural gas and ethanol are presented in Figure 7.

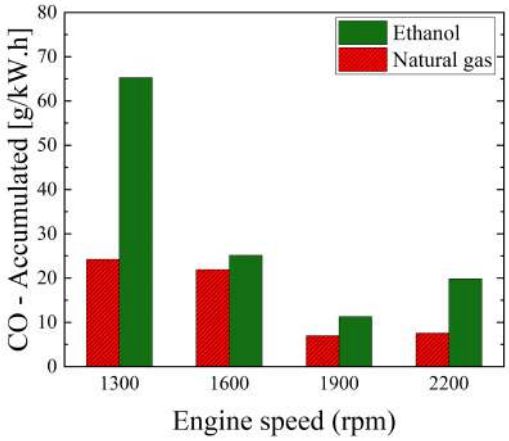

Figure 7. CO emissions from the engine operating on natural gas and ethanol.

The formation of CO during combustion is influenced by various factors, including the air-fuel ratio, combustion efficiency, and chemical characteristics of the fuel (Yücesu *et al.*, 2006), (Aldhaidhawi *et al.*, 2020). At low speeds, the burning rate may be slower, resulting in less efficient combustion and consequently higher CO emissions. As the engine speed increases and the burning rate is accelerated, there is a reduction in CO emissions, as described by the observed trend for both fuels. It is important to consider that the simulation results may be influenced by the fact that the engine was originally designed to operate with natural gas. Therefore, its operation may exhibit combustion characteristics optimized for this type of fuel, resulting in more complete combustion and consequently lower CO emissions.

5. CONCLUSIONS.

This work presents an analysis of the performance and emissions of a Vortec 3.0 (LW6) engine operating on natural gas and ethanol. For this purpose, 0D/1D simulations were conducted using the computational software AVL BOOST™ . The main conclusions of the study are as follows:

- Under the same compression ratio, the engine operating on natural gas exhibited lower output power compared to ethanol. This behavior can be attributed to the air displacement caused by natural gas in the intake manifold, which reduces the volumetric efficiency of the engine and, consequently, the energy density per injected charge into the cylinder;
- Numerically, the use of ethanol resulted in an increase in specific fuel consumption compared to natural gas. This increase is due to the lower heating value of ethanol and the lower air/fuel ratio;
- Overall, the use of ethanol led to a reduction in NO_X emissions across the entire analyzed rotational range due to lower combustion temperatures. However, higher emissions of HC and CO were observed, reflecting lower combustion efficiency.
- Although HC and CO emissions from the ethanol engine showed an increase compared to the natural gas engine, it is important to note that the use of ethanol enabled a higher power output. Therefore, improving the operating conditions of the ethanol engine, including the amount of fuel injected, the location of the injector, among other factors, could allow an adequate balance between performance and pollutant emissions. However, this will be a research topic for future work.

6. ACKNOWLEDGEMENTS

The authors acknowledge the AVL AST University Partnership Program (UPP) for the use and support of AVL-AST software., Also the authors would like to acknowledge to the UFSC Joinville IT (Mr. Kleber Carlos Francisco) team for all support given to the LABMCI computer network. The first author acknowledges the financial support granted by the *Coordenação de Aperfeiçoamento de Pessoal de Nível Superior - Brasil* (CAPES) Doctoral Fellowship Process No. 88887.686996/2022-00.

7. REFERENCES

Aldhaidhawi, M., Naji, M. and Subhi, K.A., 2020. "Numerical study of combustion characteristic, performance and emissions of a si engine running on gasoline, ethanol and lpg". *Test engineering and management*, Vol. 82, pp. 3559–3565.

Amaral, L.V., Santos, N.D.S.A., Roso, V.R., de Oliveira Sebastião, R.d.C. and Pujatti, F.J.P., 2021. "Effects of gasoline composition on engine performance, exhaust gases and operational costs". *Renewable and Sustainable Energy Reviews*, Vol. 135, p. 110196.

Aslam, M., Masjuki, H., Kalam, M., Abdesselam, H., Mahlia, T. and Amalina, M., 2006. "An experimental investigation of cng as an alternative fuel for a retrofitted gasoline vehicle". *Fuel*, Vol. 85, No. 5-6, pp. 717–724.

AVL, 2023. *AVL BOOST™ – Theory*. AVL AST.

Balki, M.K., Sayin, C. and Canakci, M., 2014. "The effect of different alcohol fuels on the performance, emission and combustion characteristics of a gasoline engine". *Fuel*, Vol. 115, pp. 901–906.

Celik, M.B., 2008. "Experimental determination of suitable ethanol–gasoline blend rate at high compression ratio for gasoline engine". *Applied Thermal Engineering*, Vol. 28, No. 5-6, pp. 396–404.

GASMIG, 2023. "Chemical composition of natural gas". https://gasmig.com.br/composicao/. Accessed June 20 2023.

Geok, H.H., Mohamad, T.I., Abdullah, S., Ali, Y., Shamsudeen, A. and Adril, E., 2009. "Experimental investigation of performance and emission of a sequential port injection natural gas engine". *European Journal of Scientific Research*, Vol. 30, No. 2, pp. 204–214.

Heywood, J.B., 2018. *Internal combustion engine fundamentals*. McGraw-Hill Education.

Iliev, S., 2015. "A comparison of ethanol and methanol blending with gasoline using a 1-d engine model". *Procedia Engineering*, Vol. 100, pp. 1013–1022.

Jahirul, M.I., Masjuki, H.H., Saidur, R., Kalam, M., Jayed, M. and Wazed, M., 2010. "Comparative engine performance and emission analysis of cng and gasoline in a retrofitted car engine". *Applied Thermal Engineering*, Vol. 30, No. 14-15, pp. 2219–2226.

Kesgin, U., 2004. "Genetic algorithm and artificial neural network for engine optimisation of efficiency and nox emission". *Fuel*, Vol. 83, No. 7-8, pp. 885–895.

Kustanto, M.N., Wardana, I.N.G., Sasongko, M.N. and Yuliati, L., 2017. "Laminar burning velocity of ethanol premixed combustion enriched with liquefied petroleum gas (lpg)". *Energetika*, Vol. 63, No. 1.

Liu, J. and Dumitrescu, C.E., 2019. "Single and double wiebe function combustion model for a heavy-duty diesel engine retrofitted to natural-gas spark-ignition". *Applied energy*, Vol. 248, pp. 95–103.

Marinov, N.M., 1999. "A detailed chemical kinetic model for high temperature ethanol oxidation". *International journal of chemical kinetics*, Vol. 31, No. 3, pp. 183–220.

Masum, B., Masjuki, H., Kalam, M., Fattah, I.R., Palash, S. and Abedin, M., 2013. "Effect of ethanol–gasoline blend on nox emission in si engine". *Renewable and Sustainable Energy Reviews*, Vol. 24, pp. 209–222.

Niculae, A.L., Miron, L. and Chiriac, R., 2020. "On the possibility to simulate the operation of a si engine using alternative gaseous fuels". *Energy Reports*, Vol. 6, pp. 167–176.

Noske, G., 1988. *Ein quasidimensionales Modell zur Beschreibung des ottomotorischen Verbrennungsablaufes*. VDI-Verlag.

Onorati, A., Ferrari, G. and D'Errico, G., 2001. "1d unsteady flows with chemical reactions in the exhaust duct-system of si engines: predictions and experiments". *SAE Transactions*, pp. 738–752.

Pattas, K. and Häfner, G., 1973. "Stickoxidbildung bei der ottomotorischen verbrennung". *MOTORTECHN. Z.*, Vol. 34, No. 12.

Patton, K.J., Nitschke, R.G. and Heywood, J.B., 1989. "Development and evaluation of a friction model for spark-ignition engines". *SAE Transactions*, pp. 1441–1461.

Poudel, S. and Deb, D., 2017. "Study of modified internal combustion engine to run with ethanol". *International Journal of Engineering and Applied Sciences*, Vol. 4, No. 8, p. 257403.

Ran, Z., Hariharan, D., Lawler, B. and Mamalis, S., 2019. "Experimental study of lean spark ignition combustion using gasoline, ethanol, natural gas, and syngas". *Fuel*, Vol. 235, pp. 530–537.

Ran, Z., Hariharan, D., Lawler, B. and Mamalis, S., 2020. "Exploring the potential of ethanol, cng, and syngas as fuels for lean spark-ignition combustion-an experimental study". *Energy*, Vol. 191, p. 116520.

Rufino, C.H., Gallo, W.L. and Ferreira, J.V., 2021. "Diagnosis of hydrous ethanol combustion in a spark-ignition engine". *Proceedings of the Institution of Mechanical Engineers, Part D: Journal of Automobile Engineering*, Vol. 235, No. 1, pp. 245–259.

Semin, R.A.B., 2008. "A technical review of compressed natural gas as an alternative fuel for internal combustion engines". *Am. J. Eng. Appl. Sci*, Vol. 1, No. 4, pp. 302–311.

STATISTA, 2023. "greenhouse gas emissions worldwide from 2015 to 2021". https://www.statista.com/statistics/1200873/intel-greenhouse-gas-emissions-worldwide/. Accessed June 10 2023.

UCSD, 2016. "San diego mechanism". https://web.eng.ucsd.edu/mae/groups/combustion/mechanism.html. Accessed June 05 2023.

Yücesu, H.S., Topgül, T., Cinar, C. and Okur, M., 2006. "Effect of ethanol–gasoline blends on engine performance and exhaust emissions in different compression ratios". *Applied thermal engineering*, Vol. 26, No. 17-18, pp. 2272–2278.

8. RESPONSIBILITY NOTICE

The authors are solely responsible for the printed material included in this paper.